Design of a bi-segmented soft actuator with hardware encoded quasi-static inflation sequence

Edoardo Milana[1], Benjamin Gorissen[1], Michaël De Volder[1,2] and Dominiek Reynaerts[1]

***Abstract*— A soft actuator composed of two fluidic bending segments is designed and manufactured having a mechanically programmed sequence of inflation. The sequence is determined by analyzing the equilibrium states between the connected segments at each step of the inflation. To do this, segments are described using their inner pressure vs. volume expansion relationship. Since it may be difficult to formulate this expression analytically for complex soft inflatable structures, an approach based on nonlinear FEM simulations is here introduced: by modelling the inner cavity of an actuator as filled with incompressible fluid and generating a fluid flux during the simulation, the pressure-volume curve is easily obtained, even if highly nonlinear. The resulting nonlinearities are instrumental in generating inflation sequencing of multiple segmented actuators, which is an example of hardware-based intelligence. Exploiting these behaviours will greatly enhance the possibilities and performances of soft robots.**

I. Introduction

Conventional robots flourished in an industrial setting where their introduction has radically changed automation and manufacturing industries. However, there are tasks where these discrete jointed robots typically fail, such as grasping a delicate object or performing complex minimally invasive surgery [1]. More generally, the so-called hard robots have difficulties in operating in close contact with living organism, as they require intricate control schemes with software encoded compliance in order not to be harmful. In this sense, soft robots are replacing or assisting hard robots in the aforementioned tasks due to their unique softness and compliancy [2]. If a soft structure collides unintentionally against another object, the energy is mechanically absorbed by the soft structure itself, making the robot intrinsically safe [3]. This inherent safety is a key attribute that distinguishes them from conventional robots, as well as their low cost and ease in manufacturing. On the other hand, there are still a lot of challenges to face, particularly on the control side. Standard control schemes are hard to implement due to the infinite degrees of freedom, as well as the need of using flexible electronics [4]. Accordingly, the attention is shifting from traditional ?software? intelligence to ?hardware? intelligence, where the functionalities are mechanically programmed in the structural design. A widely used type of soft actuators are the Elastic Inflatable Actuators (EIAs), where a pressurized fluid exerts a force on a surrounding flexible structure that transforms it into a useful global deformation [5]. EIAs with complex deformations can be designed by using the multiple segments approach, already proposed by Suzumori [6] and adopted by Overvelde [7] and Connolly [8]; namely, a complex actuator is the result of a combination of two or more simple actuators, each one considered as a building-block segment. Driving the inflations sequence of the segments leads to the desired kinematic trajectory. In order to mechanically program the inflations sequence, a design and modeling tool is required. A fundamental element for such a tool is the the relationship between inner pressure and deformation, which fully characterizes the mechanical behavior of a single EIA. Since EIAs are made out of rubbery materials, the resulting nonlinear hyperelastic models [9] are not easily formulated analytically. Therefore the design is often based on empirical assumptions and trial and error [10]. Nevertheless, hyperelastic models of inflatable structures have been developed for spherical and cylindrical balloons [11], whose geometrical symmetry simplifies the equations and allows to express the pressure in function of the stretch or volume expansions. Although there are some examples in literature that use spherical balloons [7] [12], most EIAs have more intricate shapes to achieve bending or twisting motions [13] [14], leading to an increase in model complexity. This complexity can be reduced by incorporating a fiber-reinforced design [15], where surrounding fibers hinder the cross-sectional deformation, allowing to neglect circumferential strains. For these actuators the relationship between pressure and deformation is almost linear, and when connected in a multiple segments approach, their inflation rate remains constant, prohibiting any sequence. In contrast, interconnected spherical balloons, due to the strong nonlinearity of their pressure-volume curves [9], inflate quasi-statically in a certain sequence and moreover, the sequence can change during the deflation due to snap-through instabilities, causing the actuator to follow different trajectories between loading and unloading. This paper will use the concept of sequencing originally developed for spherical balloons and extend it to all types of EIAs. Where this paper discloses the theory for an inflatable structure consisting of two segments, it can analogously be broadened to multiple segments. As such, this principle can be used in applications where sequencing is paramount but where valves and supply tubes are to be avoided and replaced by a thorough design of the actuators themselves. A first precondition for hardware sequencing is to determine the pressure-volume relationship (PV curve) of the desired inflatable actuator, which has to be preferably nonlinear,

[1]Edoardo Milana, Benjamin Gorissen, Michaël De Volder and Dominiek Reynaerts are with the Department of Mechanical Engineering, KU Leuven, Members Flanders Make, Leuven, Belgium edoardo.milana@kuleuven.be

[2]Michaël De Volder is also with the Institute for Manufacturing, Dept. Of Engineering University of Cambridge Cambridge, UK

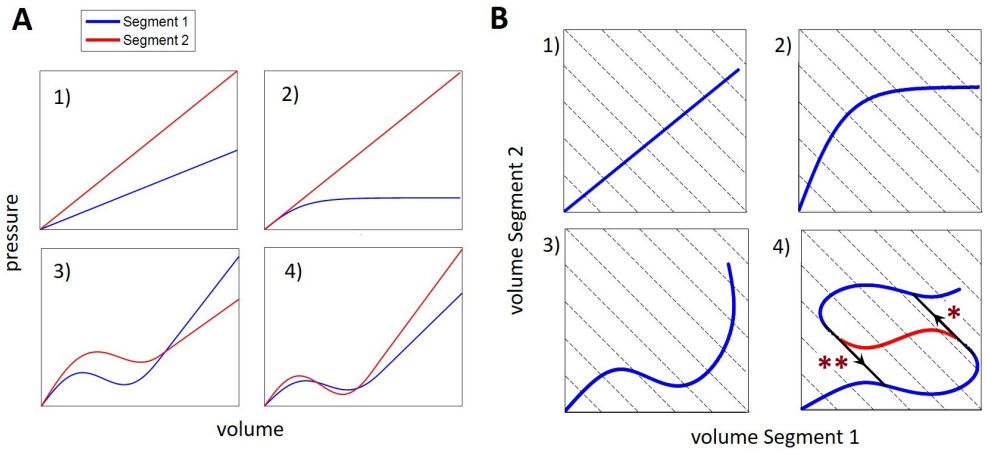

Fig. 1. A) PV curves of two segments for the cases of 1) no sequence, 2) partial sequence, 3) symmetric sequence, 4) asymmetric sequence. B) Resulting distribution of the volumes in the four cases, in blue the stable configurations, in red the instable; (*) represents the snap-through instability during inflation and (**) during deflation.

as will be made clear further. Although EIAs have been widely described using a pressure vs deformation graph, PV-characterizations have been largely omitted in literature, with only a few experimentally measured relations [10], [16]. This paper will report on a new method to calculate the PV-curve of inflatable actuators by using the commercial nonlinear FEM code Abaqus. This relation will be used to mechanically program the inflation sequence of a multi-segmented actuator system based on an energetic approach. In this way, the deformation and trajectory of a multi-segmented actuator is calculated based on the equilibrium configurations of each segment. In a first section, a general analytical model of two interconnected elastic inflatable actuators is described based on their individual PV curves. Thanks to this model, it is possible to calculate how the total volume is distributed between the segments at each loading step and if there is an inflation/deflation sequence. Subsequently, the PV curves of the designed bending actuators are calculated with Abaqus and implemented in the analytical model. These results are then validated using FEM simulation and experimental measurements on a bi-segmented actuator demonstrator.

II. Design and Modelling

A. Analytical model of bi-segmented soft actuators

The model here presented, based on [7], is valid for any kind of soft actuator composed by two segments, where each segment is considered to be an EIA with a certain deformation. Each EIA is characterized by a pressure vs. volume curve. When two segments are interconnected, the PV characteristics of the composed actuator can be calculated with the assumption that the total volume is the sum of the two volumes and the pressure is the same for the two segments:

$$p(v) = p_1(v_1) = p_2(v_2) \tag{1}$$

$$v = v_1 + v_2 \tag{2}$$

The elastic energy stored (E) is defined as the sum of the elastic energies of the two segments. V_1 and V_2 are the initial volumes:

$$E(v_1, v_2) = E_1(v_1) + E_2(v_2) = \int_{V_1}^{v_1} p_1(v)dv + \int_{V_2}^{v_2} p_2(v)dv \tag{3}$$

By using (2), it is possible to obtain the following relation:

$$\int_{V_2}^{v_2} p_2(v)dv = \int_{V_2}^{v-v_1} p_2(v)dv \tag{4}$$

Then, (3) can be written in function of one parameter:

$$E(v_1) = \int_{V_1}^{v_1} p_1(v)dv + \int_{V_2}^{v-v_1} p_2(v)dv \tag{5}$$

After derivation, (5) can be used together with (1) to form:

$$\frac{dE}{dv_1} = p_1(v_1) - p_2(v - v_1) = 0 \tag{6}$$

Equation (6) means that the configuration of the soft actuator at a certain volume corresponds to an equilibrium situation between the two segments. If the stationary point resulting from (6) is a local maximum or minimum, the configuration is unstable or stable. This analysis also determines how the total volume is distributed between the two segments at each inflation step, where the inflation history will also be a determining factor as will be shown further. Based on the shape of the individual PV curves, shown on Figure 1A, different inflation/deflation scenarios of a bi-segmented actuator can be distinguished. These sequences are more clearly depicted at Figure 1B, where for each loading step, the volume distribution v_1 vs. v_2 is plotted. If this equilibrium is stable, it is showed in blue, while unstable equilibria are colored red. For a total volume v, the equilibrium position can be found by looking at the intersection between the input volume line, which is a straight line going through $v_1 = v$ and $v_2 = v$, and the loading line, which is the blue/red graph. Thus, an inflation in these graphs is represented by moving the input volume line upwards while deflation moves it downwards. As such, 4 different sequences can be distinguished (Figure 1):

1) No sequence: When the PV curves are both linear, the distribution of the volumes is also linear and the segments inflate together, without a varying rate.

2) Partial sequence: When one PV curve shows a plateau at a certain pressure, the segments will initially inflate together while after a certain injected volume the inflation is primarily directed towards one segment while the other remains in his state or inflates at a considerable reduced rate.

3) Symmetric sequence: In this type of sequencing there is a certain inflation order that is symmetric, meaning that inflation and deflation follow the same path in the v_1- v_2 curve. This behavior occurs when at least one of the PV curves shows a pressure peak. As such, the inflation is first directed towards one segment, while after a certain total volume the inflation is directed towards the other segment.

4) Asymmetric sequence: For this type, inflation and deflation follow a different path in the v_1-v_2 curve. This behavior emerges for instance when both segments incorporate a pressure peak and a valley, where the one with the highest peak also has the lowest valley. As such the v_1-v_2 curve shows an unstable regions that triggers a snap-through instability during inflation (*) and a different one during deflation (**). When these snap-through phenomena occur, a fast exchange of fluid between the two segments can be observed which is instrumental in the design of actuator sequencing.

B. Dimensioning the segments

The bi-segmented soft actuator analyzed in this work is composed by two bending EIAs, whose inflation follows the partial sequence scenario. One segment is designed to have a preferential inflation compared to the other. The segment that inflates more is placed as tip of the actuator and it is named "top segment"; the other segment at the base is called "bottom segment". The idea is to have a two-phases motion: first, the two segments bend towards the same direction causing the entire structure to move, subsequently, only the top segment continues to bend, curling over itself like an octopus tentacle. The geometry adopted is planar with a square cross-section. A regular pattern of alternate walls and membranes is defined on one side of the actuator; the other side is composed by a thick rubber beam to achieve the cross-sectional asymmetry needed for the actuator to bend [17]. By varying the wall thickness and membrane dimensions, the two segments are tuned in order to meet the PV requirements to accomplish the partial sequence. The final dimensions are reported in Table 1 and showed in Figure 2.

TABLE I
SOFT ACTUATOR DIMENSIONS

Feature	Values (mm)
Soft actuator	
Actuator length (L)	222
Actuator height (h)	15
Actuator width (w)	15
Beam thickness (e)	5
Inner cavity width (g)	11
Wall length (a)	4
Membrane length (b)	6
Bottom segment	
Membrane thickness (t_b)	1
Wall thickness (d_b)	1
Top segment	
Membrane thickness (t_t)	0.5
Wall thickness (d_t)	2

C. Nonlinear FEM simulation of the two segments

The deformation of the two bending EIAs is simulated using the commercial FEM program, Abaqus, in the Implicit Static mode. The actuators are made out of Ecoflex 00-30, a material which is extensively adopted in soft robotics [18] due to its softness (Shore 00-30) and high elongation at break (900%) [19]. An hyperelastic Arruda-Boyce model is implemented, with the parameters already measured by Martinez et al. [16]. Instead of virtually loading the actuators

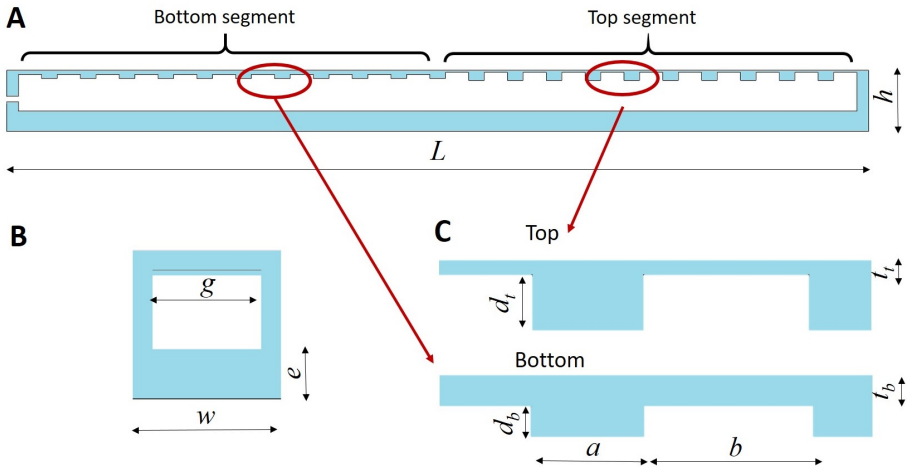

Fig. 2. A) soft actuator lateral view showing the two segments. B) soft actuator cross section. C) details of the regular pattern of membranes and walls for the two segments.

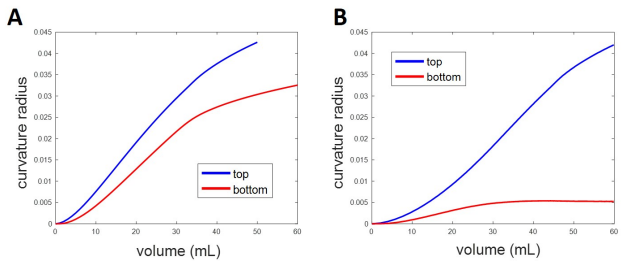

Fig. 3. A) Volume and curvature radius relationship for the two segments. B) Total volume and curvature radius for the two segments when interconnected during inflation.

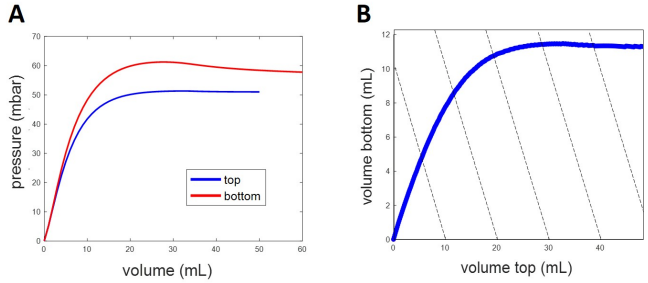

Fig. 4. A) Segments PV curves calculated with Abaqus. B)Volume distribution among the two segments interconnected during inflation calculated with the analytical model.

with a pressure ramp, as normally reported in literature [20], a novel approach is used, in order to easily obtain the PV curve and simulate nonlinear behaviors. The inner chamber is treated as a fluidic cavity filled with an incompressible fluid, through the Abaqus option *FLUID CAVITY. At each step of pseudo-time the volume of fluid is increased (option *FLUID FLUX), causing the structure to deform and exert a pressure on the cavity. Given a volume ramp as input, the pressure is thus an output which can follow any nonlinear path, leading to more numerical stability. Pressure and volume of the fluidic cavity are automatically calculated by Abaqus for each step. The two segments are separately simulated using this approach: both PV plots and the curvature radii variation are calculated during the volume ramp (Figure 3A and 4A). Top segment reaches a plateau at a lower pressure than the bottom segment, triggering its preferential inflation. It is also interesting to note that the curvature radius is almost directly proportional to the volume, at least for most of the inflation.

D. Calculation of the inflation sequence

In order to compute the inflation sequence and trajectory of the combined actuator, the two PV curves and curvature radii are imported in an assembling algorithm based on the analytical model of paragraph A). As such, combinations of actuator segments can be rapidly computed analytically, while the time-consuming simulations need to be performed only once per segment. The distribution of volume for the combination of the aforementioned segments is shown in Figure 3B and 4B: at the beginning both segments inflate, while after a certain total volume, the inflation is directed towards the top segment. According to this design, the whole actuator starts bending until a certain point where only the top segment curls further while the bottom segment remains nearly stationary.

III. Soft Actuator Manufacturing

The bi-segmented soft actuator is manufactured with a soft lithography process. Two 3-D printed (Objet30 Prime Stratasys) molds are made: one containing the membrane features of the inner cavity and the other containing the thick layer. The molds are filled with the liquid Ecoflex 00-30 polymer (two components A and B, mixed in a ratio 1:1) and placed in the oven at 70 °C for 10 minutes. The parts are then peeled-off and bonded together using the same polymer as glue. A needle is inserted in the actuator as fluidic connection. The overview of the process is depicted in Figure 5.

IV. Results

The analytical assembling of the segments is compared to a FEM simulation of the entire bi-segmented actuator and to experimental results: Figure 7 reports five inflation steps showing the correspondence of the trajectories.

A. Nonlinear FEM simulation

A nonlinear simulation of the bi-segmented actuator is executed with Abaqus. This simulation has been done using the same FEM protocol as for the single segments, with results shown on Figure 6A in terms of overall PV curve (dashed line) and on figure 7B in terms of deformation. These results are to be compared to the analytical model, that used the combined FEM simulated results of the single segments, which are shown on Figure 6A (solid line) and figure 7A. As can be seen, the analytical results match well with the FEM results, except some discrepancies in deformation at the highest volumes: at that point of the simulation (Figure 7B at step 5) the top segment is not bending with a constant radius, which implicitly is assumed in the curvature vs pressure output that is used in the deformation analysis. It is relevant to note that the time required for the assembling algorithm to perform the results is significantly shorter than the Abaqus simulation of the bi-segmented actuator.

B. Experimental measurements

The PV curve (Figure 6B) of the demonstrator actuator is measured by transferring continuously a controlled amount of incompressible fluid (water) with a syringe pump at 0.05

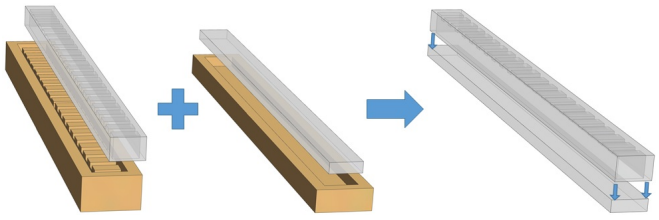

Fig. 5. The two molds (light brown) and the two parts (transparent grey) glued together.

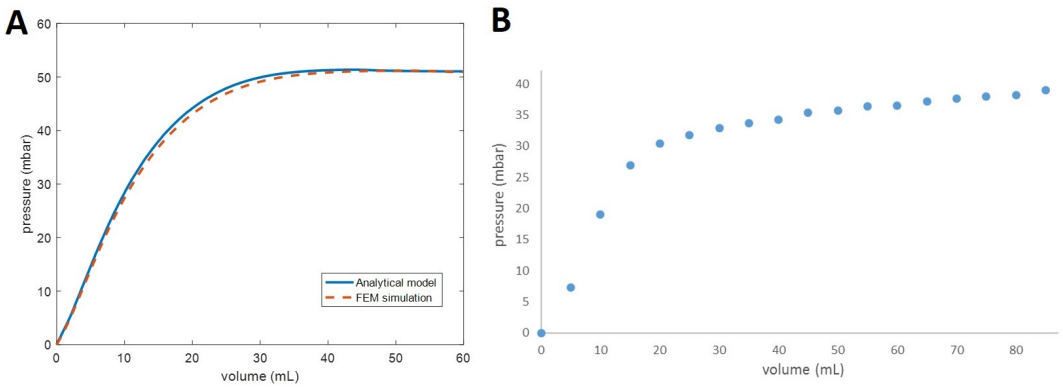

Fig. 6. PV curves of the bi-segmented actuator. A) Comparison between the FEM simulation and the analytical assembling of the segments. B) Experimental curve measured for the manufactured actuator.

mL/s. These experimental conditions resemble the loading approach (fluid flux in a fluid cavity) used in simulations. In order to minimize the effect of gravitational forces, the actuator is immerged in water during the characterization. At certain intervals camera pictures are taken of the deformation of the actuator, as can be seen on Figure 7C. These pictures show that the actuator indeed exhibits a partial sequence characteristic: at first both segments are bending while from a certain point (step 3) only the top segment continues its curling motion. When comparing the actuator deformation between simulations and experiment, the actual actuator needs more volume to obtain the same curvature after a certain volume: in Figure 7, steps 3, 4, 5 correspond to 25, 45 and 60 mL in the simulations and 30, 50, 65 mL in the experiment. It can be seen in the experiment that, from step 3, there are some membranes on the side of the actuator that are inflating more than others, producing this increase of volume. Most likely, this behavior is caused by little variations of the membranes thicknesses due to imperfections in the molds. Further, the prototype of the bi-segmented actuator achieves partial sequencing even if it presents some differences with the simulations (Figure 6) in terms of pressure values and shape. While in the simulation a perfect plateau is reached already at 40 mL, this plateau is replaced with a slight

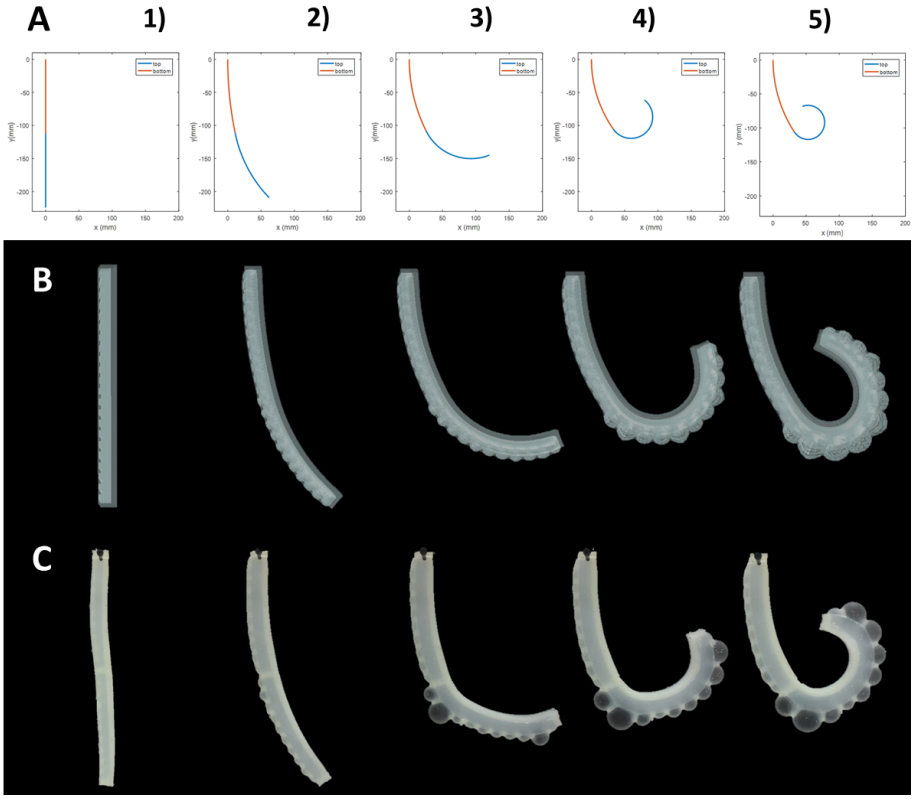

Fig. 7. Bi-segmented soft actuator trajectory comparison of analytical model (A), Abaqus simulation (B) and experimental test (c).

slope in the experiments. This mismatch can be explained by not perfectly fitting the material parameters with the experimental conditions, since the mechanical properties of Ecoflex depend on several criteria like mixing ratio, curing temperature and time. However, the prototype, accordingly to the simulation and the model, shows a change in the inflation rate of the segments and a preferential actuation of the tip, validating the mechanically programmed design.

V. Conclusion

The analytical model based on equilibrium configurations of interconnected segments has been applied successfully to the design of a soft actuator with a mechanically programmed inflation sequence. The method to calculate the PV curves of Elastic Inflatable Actuators with FEM shows reliable results and supplies an alternative to analytical modelling. Simulating the single segments and assembling them according to the equilibrium configurations gave the same results as simulating the entire multi-segmented actuator using FEM. However, it is computationally faster to calculate the energetic configurations rather than perform a FEM simulation of the total actuator. Once a library of segments and PV curves is obtained, the advantage of having an assembling algorithm becomes relevant: already from a cluster of 3 basic EIAs, 9 different bi-structured actuators can be assembled, reducing the number of FEM simulations needed by a quadratic factor. Moreover, the model provides insights into the distribution of volumes and, thus, the quasi-static inflation sequence, which is a paradigm of how hardware intelligence can be achieved in soft robots.

Acknowledgment

This research is supported by the Fund for Scientific Research-Flanders (FWO), and the European Research Council (ERC starting grant HIENA).

References

[1] C. Majidi, "Soft Robotics: A Perspective ?Current Trends and Prospects for the Future," *Soft Robotics*, vol. 1, no. 1, pp. 5–11, 2013.
[2] B. Trimmer and G. Whitesides, "An Interview with George Whitesides," *Soft Robotics*, vol. 1, no. 4, pp. 233–235, 2014. [Online].
[3] B. Trimmer, "Soft robots," pp. R639–R641, 2013.
[4] D. Rus and M. T. Tolley, "Design, fabrication and control of soft robots," *Nature*, vol. 521, no. 7553, pp. 467–475, may 2015.
[5] B. Gorissen, D. Reynaerts, S. Konishi, K. Yoshida, J.-W. Kim, and M. De Volder, "Elastic Inflatable Actuators for Soft Robotic Applications," *Advanced Materials*, p. 1604977, sep 2017.
[6] K. Suzumori, S. Iikura, and H. Tanaka, "Development of flexible microactuator and its applications to robotic mechanisms," *Proceedings. 1991 IEEE International Conference on Robotics and Automation*, no. April, pp. 1622–1627, 1991.
[7] J. T. B. Overvelde, T. Kloek, J. J. a. D'haen, and K. Bertoldi, "Amplifying the response of soft actuators by harnessing snap-through instabilities." *Proceedings of the National Academy of Sciences of the United States of America*, vol. 112, no. 35, pp. 10 863–8, 2015.
[8] F. Connolly, C. J. Walsh, and K. Bertoldi, "Automatic design of fiber-reinforced soft actuators for trajectory matching," *Proceedings of the National Academy of Sciences*, p. 201615140, 2016.
[9] I. Muller, P. Strehlow, and M. Marder, "Rubber and Rubber Balloons: Paradigms of Thermodynamics," p. 55, 2005.
[10] B. Mosadegh, P. Polygerinos, C. Keplinger, S. Wennstedt, R. F. Shepherd, U. Gupta, J. Shim, K. Bertoldi, C. J. Walsh, and G. M. Whitesides, "Pneumatic networks for soft robotics that actuate rapidly," *Advanced Functional Materials*, vol. 24, no. 15, pp. 2163–2170, 2014.
[11] A. N. Gent, "Elastic instabilities in rubber," pp. 165–175, 2005.
[12] D. Glozman, N. Hassidov, M. Senesh, and M. Shoham, "A self-propelled inflatable earthworm-like endoscope actuated by single supply line," *IEEE Transactions on Biomedical Engineering*, vol. 57, no. 6, pp. 1264–1272, 2010.
[13] B. Gorissen, W. Vincentie, F. Al-Bender, D. Reynaerts, and M. De Volder, "Modeling and bonding-free fabrication of flexible fluidic microactuators with a bending motion," *J. Micromech. Microeng*, vol. 23, pp. 45 012–10, 2013
[14] B. Gorissen, T. Chishiro, S. Shimomura, D. Reynaerts, M. De Volder, and S. Konishi, "Flexible pneumatic twisting actuators and their application to tilting micromirrors," in *Sensors and Actuators, A: Physical*, vol. 216, 2014, pp. 426–431.
[15] F. Connolly, P. Polygerinos, C. J. Walsh, and K. Bertoldi, "Mechanical Programming of Soft Actuators by Varying Fiber Angle," *Soft Robotics*, vol. 2, no. 1, pp. 26–32, 2015.
[16] R. V. Martinez, J. L. Branch, C. R. Fish, L. Jin, R. F. Shepherd, R. M. D. Nunes, Z. Suo, and G. M. Whitesides, "Robotic tentacles with three-dimensional mobility based on flexible elastomers," *Advanced Materials*, vol. 25, no. 2, pp. 205–212, 2013.
[17] B. Gorissen, M. De Volder, A. De Greef, and D. Reynaerts, "Theoretical and experimental analysis of pneumatic balloon microactuators," *Sensors and Actuators, A: Physical*, vol. 168, no. 1, pp. 58–65, 2011.
[18] J. C. Case, E. L. White, and R. K. Kramer, "Soft Material Characterization for Robotic Applications," *Soft Robotics*, vol. 2, no. 2, pp. 80–87, 2015.
[19] Smooth - on, "Ecoflex ® Series," 2011. [Online].
[20] P. Moseley, J. M. Florez, H. A. Sonar, G. Agarwal, W. Curtin, and J. Paik, "Modeling, Design, and Development of Soft Pneumatic Actuators with Finite Element Method," *Advanced Engineering Materials*, vol. 18, no. 6, pp. 978–988, 2016.